Received: 28 June 2024 | Revised: 26 September 2024 | Accepted: 2 October 2024

DOI: 10.1111/nan.13012

ORIGINAL ARTICLE

Neuropathology and Applied Neurobiology
JOURNAL OF THE BRITISH NEUROPATHOLOGICAL SOCIETY

WILEY

Characterisation of the tumour microenvironment in primary and recurrent glioblastomas

Arnon Møldrup Knudsen[1,2,3] | **Jesper Dupont Ewald**[1,2] | **Vilde Pedersen**[4,5] | **Martin Haupt-Jorgensen**[4] | **Elisabeth Victoria Riber Hansen**[6] | **Bjarne Winther Kristensen**[1,2,4,5]

[1]Department of Clinical Research, University of Southern Denmark, Odense, Denmark

[2]Department of Pathology, Odense University Hospital, Odense, Denmark

[3]Department of Pathology, Aarhus University Hospital, Aarhus, Denmark

[4]Department of Pathology, Bartholin Institute, Rigshospitalet, Copenhagen University Hospital, Copenhagen, Denmark

[5]Department of Clinical Medicine and Biotech Research Innovation Center (BRIC), University of Copenhagen, Copenhagen, Denmark

[6]Department of Pathology, Zealand University Hospital, Roskilde, Denmark

Correspondence
Arnon Møldrup Knudsen, Department of Pathology, Aarhus University Hospital, Palle Juul-Jensens Boulevard 99, 8200 Aarhus N, Denmark.
Email: arnknu@rm.dk

Funding information
This study was financially supported by the University of Southern Denmark, The Danish Cancer Society and Odense University Hospital.

Abstract

Aims: Glioblastoma patients have a dismal prognosis, due to inevitable tumour recurrence and respond poorly to immunotherapy. Tumour-associated microglia/macrophages (TAMs) dominate the glioblastoma tumour microenvironment and have been implicated in tumour progression and immune evasion. Early recurrent glioblastomas contain focal reactive regions with occasional fibrosis, chronic inflammation, TAMs and tumour cells. Surgical specimens from these tumours are rare and provide crucial insights into glioblastoma recurrence biology. This study aimed to characterise TAM- and lymphocyte phenotypes in primary vs early- and late-recurrent glioblastomas.

Methods: Patient-matched primary and recurrent glioblastomas were compared between patients with early recurrences ($n = 11$, recurrence ≤6 months) and late recurrences ($n = 12$, recurrence after 12–19 months). Double-immunofluorescence stains combining Iba1 with HLA-DR, CD14, CD68, CD74, CD86, CD163, CD204 and CD206 along with stains for CD20, CD3, CD8 and FOXP3 were quantified with software-based classifiers.

Results: Reactive regions in early recurrent tumours contained more TAMs (31.4% vs 21.7%, $P = 0.01$), which showed increased expression of CD86 (59.4% vs 38.4%, $P = 0.04$), CD204 (48.5% vs 28.4%, $P = 0.03$), CD206 (25.5% vs 14.4%, $P = 0.04$) and increased staining intensity for CD163 (86.4 vs 57.7 arbitrary units, $P = 0.02$), compared to late recurring tumours. Reactive regions contained more B-lymphocytes compared to patient-matched primary tumours (0.71% vs 0.40%, $P = 0.04$). Fractions of total, cytotoxic and regulatory T-lymphocytes did not differ.

Conclusions: Early recurrent glioblastomas showed enrichment for TAMs, expressing both pro- and anti-inflammatory markers and B-lymphocytes. This may indicate a time-dependent response to immunotherapy explained by time-dependent alterations in the immune-microenvironment in recurrent glioblastomas.

KEYWORDS
glioblastoma, lymphocyte, reactive changes, recurrence, tumour microenvironment, tumour-associated microglia/macrophage

INTRODUCTION

Glioblastoma is the most common and malignant type of primary brain tumour, with a very poor median survival of ~15 months [1]. Despite maximal surgical resection followed by adjuvant concomitant radio- and chemotherapy, nearly all patients experience tumour recurrence. Glioblastoma tumour cells have an intricate communication and interplay with both vascular, immune and glial cell types in the tumour microenvironment [2], such as tumour-associated microglia/macrophages (TAMs) [3,4], reactive astrocytes [5] and T-cells [6], and thereby facilitate tumour cell survival and therapeutic resistance [7,8]. Pro-tumourigenic TAMs further recruit immuno-suppressive regulatory T-cells and myeloid-derived suppressor cells to drive tumour progression and immune evasion [9].

Glioblastoma tumour cells are characterised by their highly infiltrative nature and migrate into the surrounding brain parenchyma [10]. Residual tumour cells left in and adjacent to the resection cavity are the origin of inevitable tumour recurrence, and it is estimated that ~90% of recurrences are located in the resection margin [11]. The traumatic injury induced by surgical tumour resection induces microenvironmental secretion of interleukins (e.g. IL-1β, IL-6 and IL-8) and growth factors (e.g. basic fibroblast growth factor [bFGF], vascular endothelial growth factor [VEGF] and platelet-derived growth factor [PDGF]). These stimulate prolonged neuroinflammation and not only promote repair mechanisms but also induce tumour cell proliferation and facilitate recurrence [12]. Neuroinflammation can persist for many months and is a highly complex process resulting from activation of many non-neoplastic cell types such as intrinsic central nervous system cells (e.g. neurons, oligodendrocytes, astrocytes, microglia, pericytes and endothelial cells) and extrinsic blood-borne cells (e.g. macrophages, neutrophils, NK cells, T-cells, B-cells and thrombocytes) [13], leading to secretion of cytokines, chemokines, interleukins and growth factors [14]. Radio- and chemotherapy not only are cornerstones in glioblastoma therapy, but also induce neuroinflammation and substantial changes in the tumour microenvironment by induction of oxidative stress, hypoxia with subsequent neoangiogenesis, induction of cell death with increases in antigen presentation, astrogliosis and activation of TAMs [15–17]. Although a pro-tumourigenic role of the tumour microenvironment has been well established, not much is known about temporal phenotypic changes in the microenvironment in early recurrent glioblastomas, which are characterised by post-therapeutic inflammatory and reactive changes. The aim of this study was to investigate the phenotypic changes in the tumour microenvironment in early recurring glioblastomas with particular emphasis on TAM and lymphocyte populations.

Key Points

- Early recurrent glioblastomas contain regions with persisting reactive changes characterised by both myeloid and lymphocytic leukocyte populations, TAMs, tumour cells and varying degrees of fibrosis.
- TAMs in the reactive regions in early recurrent glioblastomas showed enrichment for both pro- and anti-inflammatory markers, highlighting complex reactive phenotypes.
- The reactive tumour regions in early recurrent glioblastomas contained significantly higher fractions of B-lymphocytes compared to the patient-matched primary tumours, whilst no changes were found among T-lymphocyte populations.

MATERIALS AND METHODS

Patient tissue inclusion

Formalin-fixed paraffin-embedded tissue sections from all consecutive glioblastoma patients diagnosed within a consecutive 14-year period, at Odense University Hospital, Region of Southern Denmark, Denmark, were reviewed to identify patients with matching primary and recurrent tumours. Patients having a primary and matching recurrent tumour within 6 months of initial diagnosis were further examined for potential inclusion. All tissue sections were reviewed by a neuropathologist (BWK), who outlined regions containing normal tumour tissue and reactive tumour regions. Reactive areas were defined as regions including glial fibrillary acidic protein (GFAP)–positive tumour cells, Iba-1-positive microglia/macrophages and the presence of acute/chronic inflammation. Some of the tumours had fibrotic tissue regions admixed with the reactive changes. Tissue blocks with insufficient material were excluded. This resulted in a final cohort of 11 patients with matching primary and early recurrent (≤6 months) glioblastomas. Of these, 2/11 had MGMT-promoter methylation and 10/11 patients were treated with the Stupp regimen, whilst the last patient received radiation only as 60 Gy/30 fractions. A second set of patients consisting of 12 glioblastomas with matched primary and recurrent tumours, of which 8/12 had MGMT-promoter methylation, with recurrence 12–19 months after initial diagnosis was included to compare early recurrent glioblastomas with glioblastomas recurring after 12 months. An illustrative summary of included tumour samples is depicted in Figure 1.

Immunohistochemistry

Tissue sections with a thickness of 3 μm were cut on a microtome, placed on glass slides and subject to deparaffinisation and heat-induced epitope retrieval (HIER) with CC1 buffer for 32 min at 100°C. After blocking of endogenous peroxidase activity, tissue sections were stained with H&E or incubated with the following antibodies: Iba1 (1:2000, Wako Pure Chemical Industries) 16 min at 36°C, GFAP (1:4000, Dako) and CD20 (Clone: L26, ready-to-use, Ventana Medical Systems) for 8 min at 36°C. Antibody detection was performed with the Optiview-DAB detection system, and nuclei were counterstained with haematoxylin. All staining was performed on the Ventana Discovery Ultra platform (Ventana Medical Systems). Two tissue multiblocks

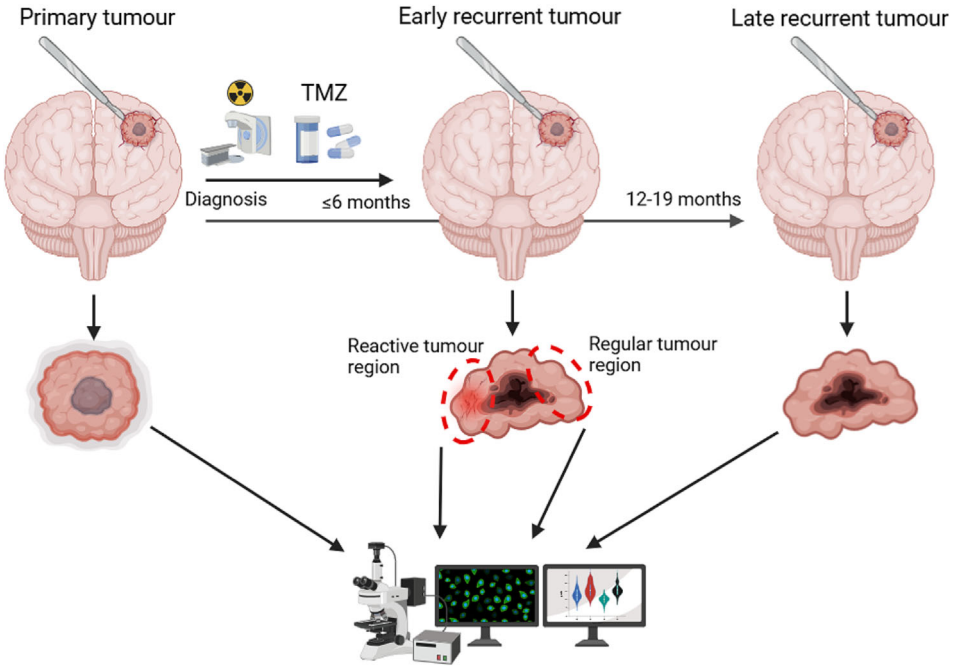

FIGURE 1 Graphic illustration of the analysed patient groups including time points for glioblastoma recurrences. Two different patient groups were established; the first group included patient-matched primary and recurrent tumours, with recurrence within 6 months after diagnosis, and the second group comprised primary tumours and recurrent tumours with recurrence 12–19 months after diagnosis. Early recurrent tumours contained both reactive and non-reactive regular tumour regions, which were segregated in the analysis to distinguish phenotypic alterations. TMZ, temozolomide.

served as negative and positive controls: one containing 27 different normal tissues plus 12 different cancers and one containing nine different glioblastomas. Stained slides were digitised using the NanoZoomer 2.0HT digital image scanner (Hamamatsu Photonics, Japan).

Double immunofluorescence staining and automated quantitative analysis

Tissue sections were prepared as previously described and incubated with the following primary antibodies: Iba1 (1:3000, Wako Pure Chemical Industries) 16 min at 36°C, CD8 (clone: C8/144B, 1:100, Dako) for 32 min at 36°C or FOXP3 (clone: 236A/E7, 1:40, Thermo Fisher Scientific) for 16 min at 36°C. Antibody detection was performed with the DISCOVERY Cy5 kit. Slides were then subject to a second round of HIER and incubated with the second primary antibodies: CD68 (clone: PG-M1, 1:50, Dako) 16 min at 36°C, CD74 (clone: LN2, 1:200, Santa Cruz) 32 min at 36°C, CD86 (1:200, R&D Systems) 60 min at 36°C, CD163 (clone: MRQ-26, Ready-to-use, Ventana Medical Systems) 8 min at 36°C, CD204 (clone: SRA-E5, 1:600, Cosmo Bio Co. LTD) 32 min at 36°C, CD206 (clone: 5C11, 1:800, Novus Biologicals) 32 min at 36°C, HLA-DR (clone: CR3/43, 1:1000, Dako), CD14 (clone: EPR3653, ready-to-use, Ventana Medical Systems), Ki-67 (clone: 8D5, 1:3000, Cell Signaling Technology) 32 min at 36°C and CD3 (clone: 2GV6, ready-to-use, Ventana Medical Systems) for 4 min at 36°C. Antibody detection was performed with the DISCOVERY FAM kit. Nuclei were counterstained with VECTASHIELD mounting medium containing DAPI.

Bright-field super images of all whole tissue sections were acquired at 1.25× magnification using the Visiopharm software (V2018.9.4) coupled with a Leica DM6000 B microscope equipped with an Olympus DP72 camera and a Ludl motorised stage. Regions of interest (ROI) including central tumour areas (both in primary and recurrent tumours) and reactive tumour areas in early recurrent tumours were manually outlined on each image. The software was set to sample 25 images at 20× magnification from each ROI using a Meander number–based sampling algorithm. Images containing necrosis, blood vessels, bleeding, staining artefacts or <20% tumour tissue in the image were excluded from the analysis. Different classifiers were designed with the Visiopharm software to measure fractions of positive cells, fractions of cells with co-expression and staining intensities of the different stains.

Statistical analysis

Different regions were compared with mixed-effects models using a restricted maximum likelihood (REML) approach and Tukey's multiple comparison tests. Multiple comparisons were performed with one-way analysis of variance (ANOVA) and subsequent Friedman test with Dunn's correction for multiple comparisons. Correlations were assessed by simple linear regression analysis. Statistical analyses were performed in GraphPad Prism V10.1.2.

RESULTS

Early recurrent glioblastomas are characterised by the presence of reactive tumour regions with distinct morphology

The initial characterisation of patient samples showed that early recurrent tumours commonly exhibited both usual tumour regions dominated by tumour cells and TAMs (Figure 2A) and, additionally, reactive tumour regions (Figure 2B,C) with distinct morphology. The reactive regions were characterised by the presence of fibroblasts and

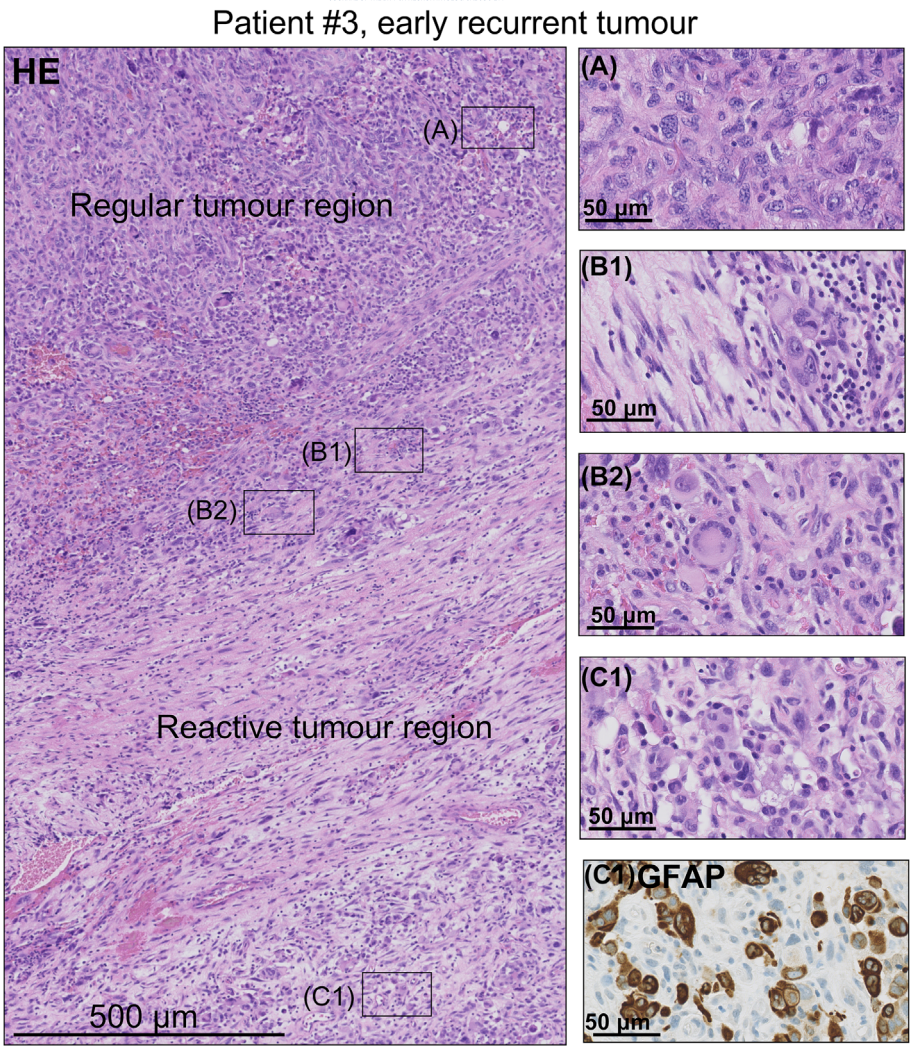

FIGURE 2 Histomorphology of reactive tumour regions in early recurrent glioblastomas. Representative HE stained tissue section from patient #3 with an early recurrent glioblastoma. (A) Display of the regular recurrent tumour region dominated by neoplastic tumour cells and TAMs. (B,C) Representation of the reactive region within the recurrent tumour characterised by fibrosis and chronic inflammation (B1 + B2) and presence of scattered neoplastic tumour cells (C1) with strong GFAP staining intensity (C2). Overview image acquired at 5× magnification, with scale bar = 500 µm. Regional images were acquired at 40× magnification with scale bars = 50 µm.

varying degrees of fibrosis (Figure 2B1), not only inflammatory cells dominated by lymphocytes but also with scattered neutrophils and multinucleated giant cell macrophages (Figure 2B2), as well as neoplastic tumour cells with strong GFAP positivity (Figure 2C1). Additional representative images from both primary tumours and patient-matched early recurrent tumours with reactive tumour regions are depicted in Figure 3, demonstrating the inclusion of GFAP-positive tumour cells and astrocytes, Iba1-positive TAMs and lymphocytes. Since both reactive astrocytes and malignant tumour cells can express GFAP, the presence of tumour cells within the reactive tumour regions in early recurrent glioblastomas was further confirmed by histomorphological evaluation and supplementary OLIG2 immunostainings. This clearly showed the presence of tumour cells characterised by enlarged and highly pleomorphic nuclei, with simultaneous expression of either GFAP or OLIG2, respectively (Figure S1A,B).

Reactive regions in early recurrent glioblastomas have higher fractions of TAMs

Next, we investigated the fractions of TAMs in matched primary and recurrent tumours. Reactive regions in early recurrent glioblastomas had a significantly higher TAM fraction compared to the patient-matched primary tumours (31.4% vs 21.7%, $P = 0.01$; Figure 4A).

We then investigated the TAM population with a series of double-immunofluorescence stains combined with automated quantitative software analysis (Figure 4B) to further characterise phenotypic distributions of TAMs among the different tumour regions. For this, the pan-TAM marker Iba1 was combined with Ki-67, CD68 and different TAM phenotype markers including classical M1-like (HLA-DR, CD14, CD74, CD86) and M2-like (CD163, CD204, CD206) proteins.

No significant differences in the fraction of proliferating TAMs ($Iba1^+/Ki\text{-}67^+$ cells) were found when comparing primary (mean = 5.3%), recurrent (mean = 3.6%) and reactive recurrent tumour regions (mean = 4.0%) in patients with early recurrence vs primary (mean = 2.7%) or recurrent regions (mean = 2.3%) in patients with late tumour recurrence (Figure 4C).

No significant differences in the $Iba1^+/CD68^+$ fractions or the CD68 staining intensities in $Iba1^+$ cells were found in the different regions in early and late recurring patients (Figure S2A,B).

The primary tumours of early recurrent patients had significantly higher fractions of TAMs expressing HLA-DR compared to primary tumours of late recurring patients (mean = 38.9% vs 18.9%,

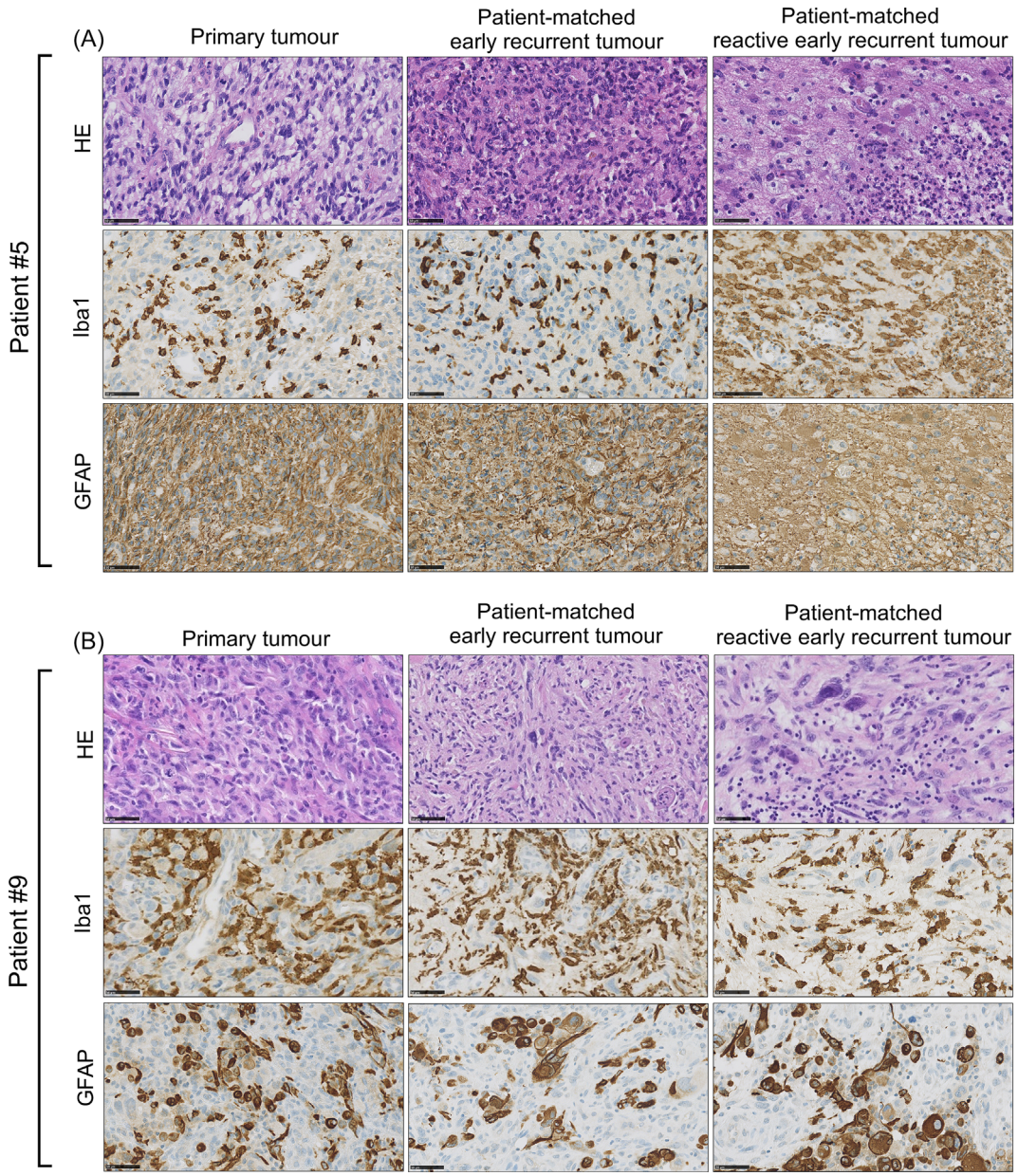

FIGURE 3 Representative morphological examples from primary tumours and the patient-matched early recurrent tumours. (A) Patient matched histological sections from both primary tumours and different regions in early recurrent tumours stained with HE, Iba1 and GFAP. Note the chronic inflammation and increased presence of Iba1$^+$ TAMs in the reactive region of recurrent tumours. (B) The reactive tumour region shows scattered lymphocytes and GFAP$^+$ tumour cells. Images were acquired at 40× magnification with scale bars = 50 μm.

$P = 0.013$; Figure 4D). No significant differences in HLA-DR staining intensity were found (Figure S2C).

When looking at the fraction and staining intensity of TAMs with expression of the M1-like markers CD14 and CD74, no significant differences were found among the different tumour regions (Figure S2D,E and S2F,G).

The recurrent tumours from patients with early recurrences had a significant increase in the fraction of TAMs expressing the pro-inflammatory M1-like marker CD86 compared to recurrent tumours from patients with late recurrences (mean = 59.4% vs 38.4%, $P = 0.04$; Figure 4E). Furthermore, the reactive recurrent region in early recurrent patients had a significantly higher CD86 staining intensity in Iba1$^+$/CD86^s cells compared to recurrent tumours from patients with late recurrences (mean = 62.6 arbitrary units [AU] vs 43.1 AU, $P = 0.04$; Figure S2H).

TAMs in early recurrent glioblastomas are enriched for pro-tumourigenic anti-inflammatory M2-like-markers

When looking at the expression of the M2-like marker CD163, there was a trend towards a higher fraction of TAMs expressing CD163 in

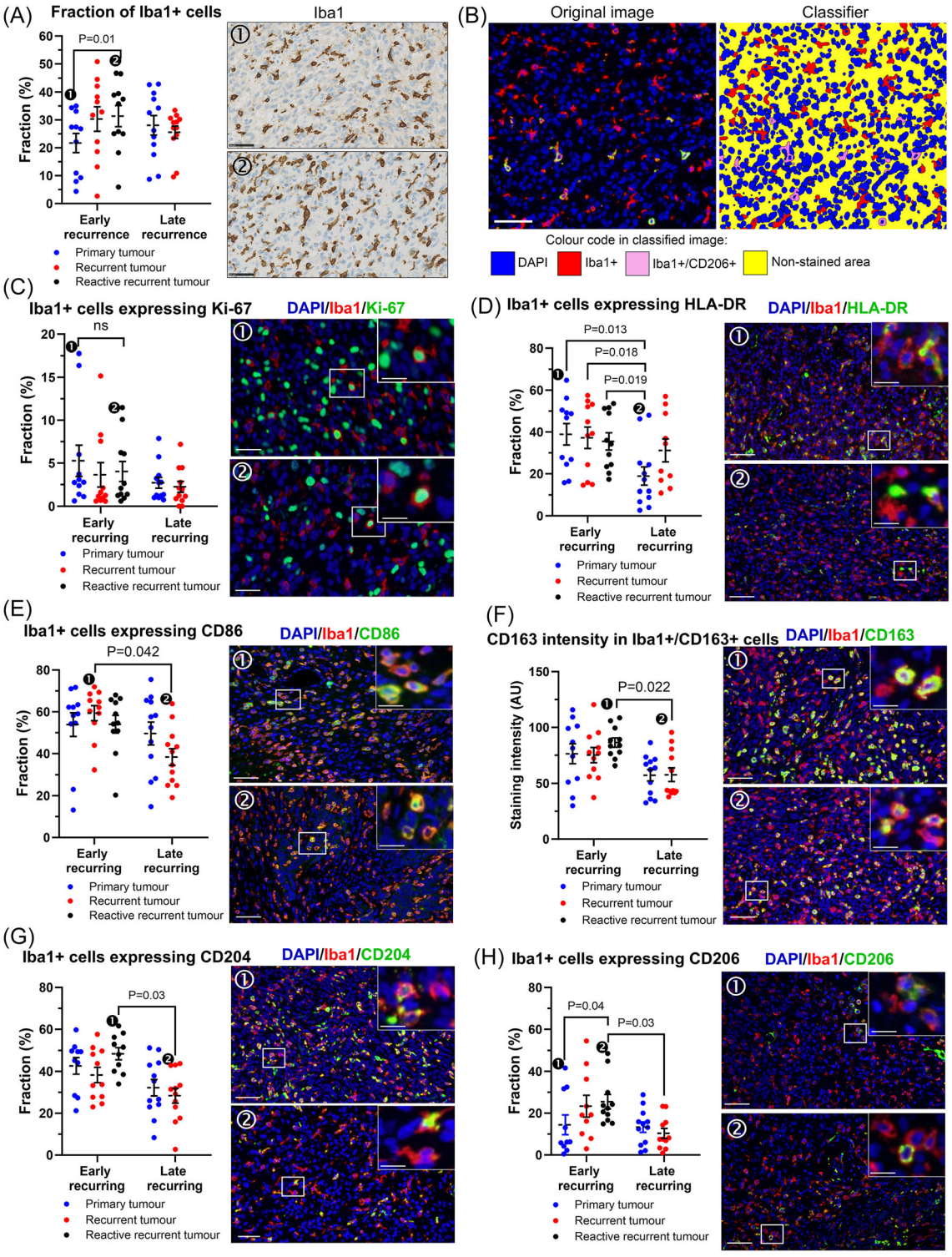

FIGURE 4 Quantification of Iba1$^+$ TAM fractions with co-expression of different phenotypic markers in primary vs recurrent tumours from patients with both early tumour recurrences and late recurrences. (A) Quantification of the Iba1$^+$ TAM fraction with representative images from primary tumour (1) and reactive regions (2) from a patient with early tumour recurrence. Scale bar = 50 µm. (B) Demonstration of a software-based classifier (in this case Iba1/CD206 quantification) designed to quantify double-immunofluorescence staining. The left image is the originally acquired image, and to the right, the classifier is overlaid on the original image. The DAPI stain represents nuclei. Scale bar = 50 µm. (C–H) Results from double-immunofluorescence quantifications with accompanying representative images. Patients with early tumour recurrence (n = 11) had three different data groups; primary tumour (blue dots), recurrent tumour (red dots) and reactive regions within the recurrent tumour (black dots) depicted as the first three entities in the graphs. Patients with late tumour recurrence had two different data groups; primary tumour (blue dots) and recurrent tumour (red dots) depicted as the last two entities in the graphs. Significant differences are shown with included p-values. Scale bars: overview images = 50 µm, inserts = 10 µm.

the reactive recurrent regions in patients with early tumour recurrence vs the recurrent tumours from patients with late recurrences (mean = 53.8% vs 37.6%, $P = 0.09$; Figure S2I). The CD163 staining intensity in Iba1$^+$/CD163$^+$ cells was significantly higher in the reactive recurrent regions in patients with early recurrences compared to the recurrent tumours of patients with late recurrences (mean 86.4 AU vs 57.7 AU, $P = 0.02$; Figure 4F).

The fraction of TAMs expressing the M2-like marker CD204 was significantly higher in the reactive recurrent regions of patients with early recurrences compared to the recurrent tumours of patients with late recurrences (mean 48.5% vs 28.4%, $P = 0.03$; Figure 4G). No differences in CD204 staining intensity in Iba1$^+$/CD204$^+$ cells were found (Figure S2J).

The fraction of TAMs with CD206 expression was significantly higher in the reactive recurrent regions compared to both the patient-matched primary tumour in patients with early tumour recurrences (mean 25.5% vs 14.4%, $P = 0.04$; Figure 4H) and when compared to the recurrent tumours from patients with late recurrences (mean 25.5% vs 10.33%, $P = 0.03$; Figure 4H). No differences in CD206 staining intensity in Iba1$^+$/CD206$^+$ cells were found in any of the different tumour regions (Figure S2K).

TAM phenotypes do not correlate with time-to-recurrence after the last dose of radiotherapy in patients with early recurrent glioblastomas

Next, we performed correlative analyses of the different TAM phenotypes and the time-to-recurrence after administration of the last radiation dose. The time-to-recurrence ranged from 2.66 to 4.82 months (median = 4.09 months; Figure S3A). No significant correlations between time-to-recurrence and the M1-like phenotypes HLA-DR and CD86 were found (Figure S3B,C), nor were there any differences when assessing both fraction and intensity for the M2-like phenotypic markers CD163, CD204 and CD206 (Figure S3D–F).

CD3$^+$ T-cells, CD3$^+$/CD8$^+$ cytotoxic T-cells and CD3$^+$/FOXP3$^+$ regulatory T-cells are equally distributed in patient-matched primary vs recurrent glioblastomas

Quantification of CD3/CD8 and CD3/FOXP3 double-immunofluorescence stains (Figure 5A,B) showed that primary tumours from patients with early tumour recurrences had a mean T-cell fraction (CD3$^+$ cells) of 1.3% (Figure 5C). No significant differences were found regarding the CD3$^+$ T-cell fraction in patient-matched recurrent (2.4% CD3$^+$ T-cells, $P = 0.46$; Figure 5C) and reactive recurrent regions (3.6% CD3$^+$ T-cells, $P = 0.13$; Figure 5C) of patients with early tumour recurrences. In patients with late tumour recurrences, the mean CD3$^+$ T-cell fraction in primary tumours was 1.3%, whilst the fraction in recurrent tumours was 1.7%, which did not significantly differ.

In patients with early recurrences, CD3$^+$/CD8$^+$ cytotoxic T-cells constituted 45.2% of total CD3$^+$ T-cells in primary tumours, 49.6% in recurrent tumours and 46.3% in reactive regions in recurrent tumours (Figure 5D). In patients with late recurrences, CD3$^+$/CD8$^+$ cells comprised 49.4% of the CD3$^+$ T-cell population in primary tumours and 49.3% in recurrent tumours (Figure 5D). No significant differences in the fractions of CD3$^+$/CD8$^+$ cytotoxic T-cells were found among the different groups. The CD3$^-$/CD8$^+$ cell population, most likely comprising NK-cells and/or monocytes, was not analysed given its very small size.

In patients with early tumour recurrences, the CD3$^+$/FOXP3$^+$ regulatory T-cell fraction comprised 6.5% of CD3$^+$ T-cells in primary tumours, 4.2% in recurrent tumours and 6.5% in the reactive regions of recurrent tumours (Figure 5E). In patients with late recurrences, CD3$^+$/FOXP3$^+$ cells comprised 12.8% of the CD3$^+$ T-cell population in primary tumours and 9.6% in recurrent tumours (Figure 5E). No significant differences were found between any of the groups.

The fraction of CD20$^+$ B-lymphocytes increases in recurrent tumours from patients with early tumour recurrence

Next, we investigated the fractions of CD20$^+$ B-lymphocytes (Figure 5F). In patients with early tumour recurrence, a trending increase in the CD20$^+$ B-lymphocyte fraction was found in recurrent tumours (mean = 0.64%, $P = 0.06$) and a significant increase was found in the reactive regions of recurrent tumours (mean = 0.71%, $P = 0.04$) compared to the patient-matched primary tumours (mean = 0.40%). This finding remained significant when looking at absolute CD20$^+$ B-lymphocyte counts ($P = 0.008$), whilst no significant changes were identified among the absolute cell numbers analysed from each tumour region (Figure 5F). In patients with late tumour recurrences, the CD20$^+$ B-lymphocyte fraction in primary (0.48%) vs recurrent (0.45%) tumours did not significantly differ (Figure 5F).

DISCUSSION

In this study, we have investigated the expression of different phenotypic M1/M2-like markers in TAMs in primary and patient-matched recurrent glioblastomas from patients with both early- and late tumour recurrences. A graphical summary of the main findings is represented in Figure 6.

Interestingly, no differences were found among the fraction of proliferating TAMs in primary vs recurrent tumours, suggesting that the majority of the identified increase of TAMs in recurrent tumours results from increased recruitment of monocytes/macrophages from the peripheral blood circulation, rather than prolonged proliferation of resident brain microglia, as also demonstrated in murine glioblastoma models [18]. In TAMs located in the reactive regions in early recurrent glioblastomas, we found a concurring increase of markers associated

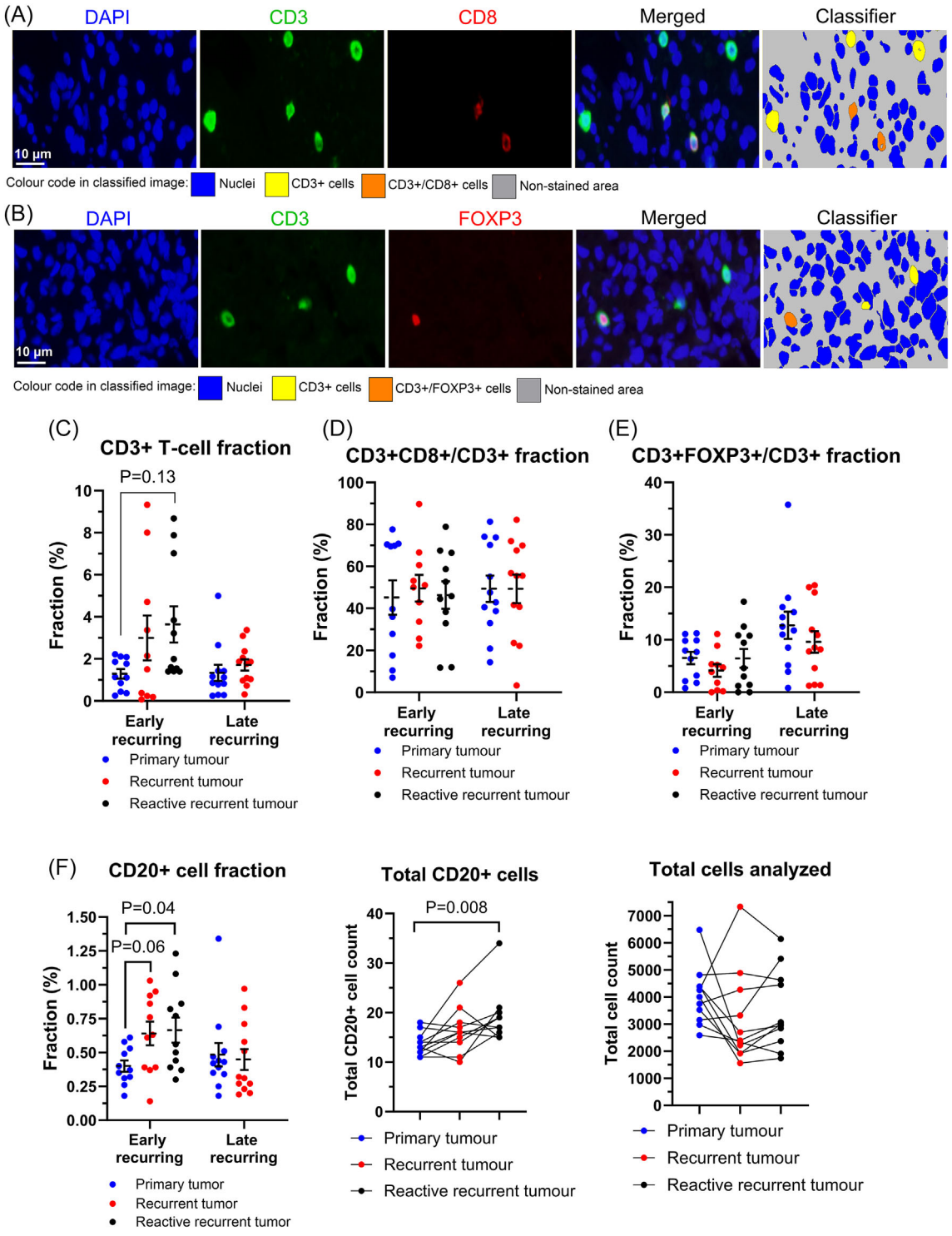

FIGURE 5 Quantification of lymphocyte populations in primary vs recurrent glioblastomas. (A, B) Representative images from CD3/CD8 and CD3/FOXP3 double-immunofluorescence stains with overlaid classifiers designed to quantify the fractions of $CD3^+/CD8^+$ cytotoxic T-lymphocytes and $CD3^+/FOXP3^+$ regulatory T-lymphocytes, respectively. Scale bars = 10 µm. (C–E) Quantifications of the different T-lymphocyte populations in the different tumour regions in patients with early- and late-recurring tumours. Results in (D) and (E) are shown as the relative $CD3^+/CD8^+$ and $CD3^+/FOXP3^+$ cell fractions respectively, divided by the total $CD3^+$ T-lymphocyte population. (F) Software-based quantification of the relative $CD20^+$ B-lymphocyte fractions and additional graphical presentation of absolute $CD20^+$ B-lymphocyte and total cell counts from each patient. Scale bar = 50 µm.

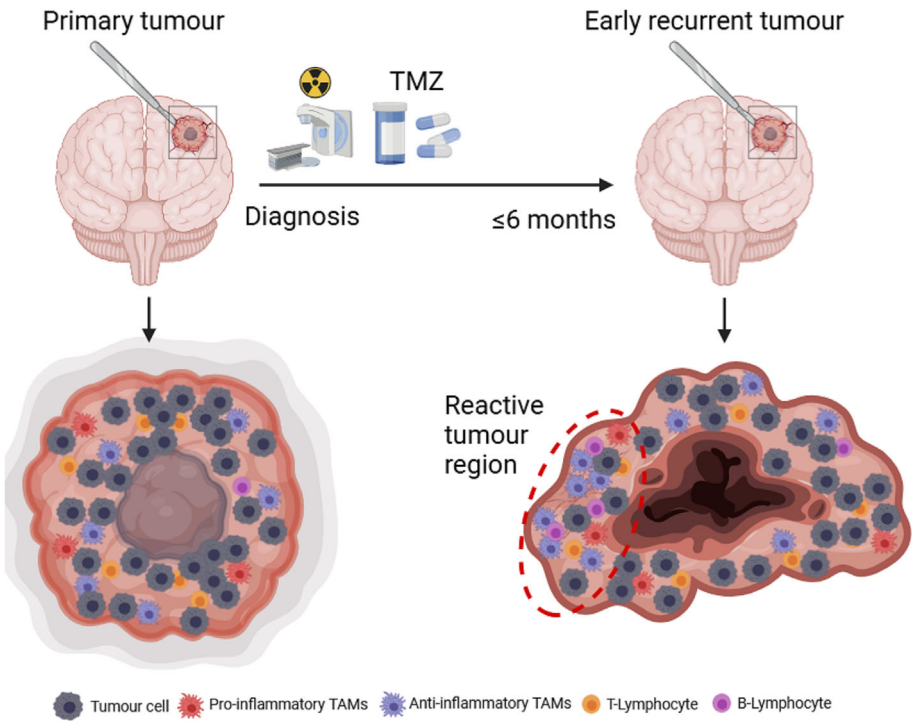

FIGURE 6 Graphical summary. Reactive regions in early recurrent glioblastomas contain TAMs enriched for expression of both pro- and anti-inflammatory markers with predominant upregulation of anti-inflammatory markers CD163, CD204 and CD206. This highlights the phenotypic complexity of the TAM populations within the reactive regions.

with both the classical pro-inflammatory M1-like phenotype (CD86) and alternatively activated anti-inflammatory tumour promoting M2-like markers (CD163, CD204 and CD206). This suggests a highly dynamic microenvironment in the reactive regions, where multiple distinct TAM phenotypes likely co-exist. The upregulation of the pro-inflammatory M1-like marker CD86 in TAMs residing in the reactive regions in early recurrent tumours implies that the inflammatory response to therapeutic interventions persists in the reactive tumour regions within the first 6 months after diagnosis. The tumour microenvironment of different cancer types has been found enriched for M2-like-polarised macrophages [19], and we demonstrate that glioblastomas are no exception to this phenomenon. In recent years, the complexity of TAM phenotypes has been greatly elucidated, partly aided by single-cell sequencing approaches, and the traditionally dichotomised M1/M2-like polarisation state of TAMs is likely an oversimplified view of TAM phenotypes. Increasing evidence suggests plasticity and co-expression of both pro- and anti-inflammatory mediators by the same TAMs, suggesting a dynamic and heterogeneous continuum of TAMs [20–23].

We found no significant differences in the fraction of $CD3^+$ T-lymphocytes nor the distribution of $CD3^+/CD8^+$ cytotoxic- and $CD3^+/FOXP3^+$-regulatory T-lymphocytes in primary vs recurrent tumours. Although no differences were found when looking at relative cell numbers/fractions, future work should look further into the characterisation of T-cell activation/exhaustion states to further shed light on T-cell functionality in the complex reactive microenvironment with abundant TAMs and evident functional cross-talk between TAMs and lymphocytes [24,25]. The increase in anti-inflammatory protein expression on TAMs in the reactive regions in early tumour recurrences could influence T-cell activation states and their anti-tumoural function, which may be of crucial relevance given the high degree of T-lymphocyte dysfunction and exhaustion in glioblastomas [6,26].

Whilst T-lymphocytes, and in particular $CD8^+$ cytotoxic T-lymphocytes, have gained tremendous attention in the past years for their pivotal role in immunotherapy [27,28], B-lymphocytes remain a relatively uncharted cell population, and their role in anticancer immunotherapy [29,30] and glioblastoma biology remains to be fully elucidated. Interestingly, we found an increase in the absolute fraction of B-lymphocytes in the reactive recurrent tumour regions. B-lymphocytes have been implicated in exosome-mediated macrophage polarisation [31] and may influence the TAM phenotype in the glioblastoma tumour microenvironment. Recently, B-lymphocytes have been associated with an immunosuppressive response towards cytotoxic T-lymphocytes mediated by myeloid-derived suppressor cell–induced expression of PD-L1 in glioblastomas, and it was further demonstrated that depletion of intratumoural regulatory B-cells could significantly prolong survival of animals with glioblastoma xenografts [32]. As such, further investigation of functional B-cell phenotypes and their implications on glioblastoma tumour biology and potential recurrence mechanisms may be warranted.

A limitation of our current study is the relatively small sample size ($n = 11$ patients) with matching primary and early recurrent (≤ 6 months) glioblastomas. Since most recurrences occur after at least 6 months, identifying sufficient numbers of suitable patients for inclusion is difficult. Our findings should therefore be validated in additional patient samples, which will most likely require multi-centre collaborations to identify sufficient numbers of patients with early recurrences.

Given the scarcity of surgical specimens from early recurrent glioblastomas, many questions regarding temporal tumour biology, and in

particular, any potential implications for therapeutic interventions including immunotherapeutic modalities, remain unanswered [33]. A deeper understanding of specific tumour microenvironmental changes in the setting of early recurrent tumours can provide valuable insights into the biology of all glioblastoma recurrences, including important insights into time-dependent alterations of the tumour microenvironment and its immune landscape. This could shed further light on potential reasons for the failure of immunotherapeutic approaches [34].

Taken together, we demonstrate that the tumour microenvironment in early recurring glioblastomas is complex and characterised by reactive regions with occasional fibrosis and chronic inflammation and showed increased expression of both classical pro-inflammatory (M1-like) and anti-inflammatory tumour-promoting (M2-like) markers in intratumoural TAMs. Early recurrent tumours showed a significantly higher fraction of B-lymphocytes, and further investigation of this cell population is warranted to uncover potential impact on glioblastoma biology and recurrence. The dynamic TAM population in recurrent glioblastomas may be implicated in immune regulation and responsiveness to immunotherapy through bi-directional interaction with local T- and B-lymphocyte populations, highlighting the complexity of the glioblastoma tumour microenvironment and its role in the recurrence process and therapeutic resistance.

CONFLICT OF INTEREST

The authors declare no conflicts of interest.

AUTHOR CONTRIBUTIONS

Study design (Arnon Møldrup Knudsen, Bjarne Winther Kristensen); data collection and analysis (Arnon Møldrup Knudsen, Jesper Dupont Ewald, Vilde Pedersen, Martin Haupt-Jorgensen, Elisabeth Victoria Riber Hansen); data interpretation (Arnon Møldrup Knudsen, Bjarne Winther Kristensen); drafting of the manuscript (Arnon Møldrup Knudsen). All authors have read and approved the final manuscript.

ACKNOWLEDGEMENTS

We would like to thank technician Helle Wohlleben for her valuable assistance with the immunohistochemical staining. This study was financially supported by the University of Southern Denmark, The Danish Cancer Society and Odense University Hospital.

PEER REVIEW

The peer review history for this article is available at https://www.webofscience.com/api/gateway/wos/peer-review/10.1111/nan.13012.

DATA AVAILABILITY STATEMENT

The data that support the findings of this study are available from the corresponding author upon reasonable request.

ETHICS STATEMENT

The study was approved by the Danish Data Inspection Authority (approval number 16/11065) and the Regional Scientific Ethical Committee of the Region of Southern Denmark (approval number S-20150148).

REFERENCES

1. Stupp R, Hegi ME, Mason WP, et al. Effects of radiotherapy with concomitant and adjuvant temozolomide versus radiotherapy alone on survival in glioblastoma in a randomised phase III study: 5-year analysis of the EORTC-NCIC trial. *Lancet Oncol*. 2009;10(5):459-466. doi:10.1016/S1470-2045(09)70025-7
2. Broekman ML, Maas SLN, Abels ER, Mempel TR, Krichevsky AM, Breakefield XO. Multidimensional communication in the microenvirons of glioblastoma. *Nat Rev Neurol*. 2018;14(8):482-495. doi:10.1038/s41582-018-0025-8
3. Morisse MC, Jouannet S, Dominguez-Villar M, Sanson M, Idbaih A. Interactions between tumor-associated macrophages and tumor cells in glioblastoma: unraveling promising targeted therapies. *Expert Rev Neurother*. 2018;18(9):729-737. doi:10.1080/14737175.2018.1510321
4. Pires-Afonso Y, Niclou SP, Michelucci A. Revealing and harnessing tumour-associated microglia/macrophage heterogeneity in glioblastoma. *Int J Mol Sci*. 2020;21(3):689. doi:10.3390/ijms21030689
5. Brandao M, Simon T, Critchley G, Giamas G. Astrocytes, the rising stars of the glioblastoma microenvironment. *Glia*. 2019;67(5):779-790. doi:10.1002/glia.23520
6. Woroniecka KI, Rhodin KE, Chongsathidkiet P, Keith KA, Fecci PE. T-cell dysfunction in glioblastoma: applying a new framework, clinical cancer research: an official journal of the American association for. *Cancer Res*. 2018;24(16):3792-3802. doi:10.1158/1078-0432.CCR-18-0047
7. Zhang X, Ding K, Wang J, Li X, Zhao P. Chemoresistance caused by the microenvironment of glioblastoma and the corresponding solutions. *Biomed Pharmacot*. 2019;109:39-46. doi:10.1016/j.biopha.2018.10.063
8. Da Ros M, De Gregorio V, Iorio AL, et al. Glioblastoma chemoresistance: the double play by microenvironment and blood-brain barrier. *Int J Mol Sci*. 2018;19(10):2879. doi:10.3390/ijms19102879
9. Chang AL, Miska J, Wainwright DA, et al. CCL2 produced by the glioma microenvironment is essential for the recruitment of regulatory T cells and myeloid-derived suppressor cells. *Cancer Res*. 2016;76(19):5671-5682. doi:10.1158/0008-5472.CAN-16-0144
10. Vollmann-Zwerenz A, Leidgens V, Feliciello G, Klein CA, Hau P. Tumor cell invasion in glioblastoma. *Int J Mol Sci*. 2020;21(6):1932. doi:10.3390/ijms21061932
11. Petrecca K, Guiot MC, Panet-Raymond V, Souhami L. Failure pattern following complete resection plus radiotherapy and temozolomide is at the resection margin in patients with glioblastoma. *J Neurooncol*. 2013;111(1):19-23. doi:10.1007/s11060-012-0983-4
12. Hamard L, Ratel D, Selek L, Berger F, van der Sanden B, Wion D. The brain tissue response to surgical injury and its possible contribution to glioma recurrence. *J Neurooncol*. 2016;128(1):1-8. doi:10.1007/s11060-016-2096-y
13. Burda JE, Sofroniew MV. Reactive gliosis and the multicellular response to CNS damage and disease. *Neuron*. 2014;81(2):229-248. doi:10.1016/j.neuron.2013.12.034
14. Mostofa AG, Punganuru SR, Madala HR, Al-Obaide M, Srivenugopal KS. The process and regulatory components of inflammation in brain oncogenesis. *Biomolecules*. 2017;7(2):34. doi:10.3390/biom7020034
15. Barker HE, Paget JT, Khan AA, Harrington KJ. The tumour microenvironment after radiotherapy: mechanisms of resistance and recurrence. *Nat Rev Cancer*. 2015;15(7):409-425. doi:10.1038/nrc3958
16. Gupta K, Burns TC. Radiation-induced alterations in the recurrent glioblastoma microenvironment: therapeutic implications. *Front Oncol*. 2018;8:503. doi:10.3389/fonc.2018.00503

17. Akkari L, Bowman RL, Tessier J, et al. Dynamic changes in glioma macrophage populations after radiotherapy reveal CSF-1R inhibition as a strategy to overcome resistance. *Sci Transl Med*. 2020;12(552). doi:10.1126/scitranslmed.aaw7843
18. Buonfiglioli A, Hambardzumyan D. Macrophages and microglia: the cerberus of glioblastoma. *Acta Neuropathol Commun*. 2021;9(1):54. doi:10.1186/s40478-021-01156-z
19. Predina J, Eruslanov E, Judy B, et al. Changes in the local tumor microenvironment in recurrent cancers may explain the failure of vaccines after surgery. *Proc Natl Acad Sci U S a*. 2013;110(5):E415-E424. doi:10.1073/pnas.1211850110
20. Müller S, Kohanbash G, Liu SJ, et al. Single-cell profiling of human gliomas reveals macrophage ontogeny as a basis for regional differences in macrophage activation in the tumor microenvironment. *Genome Biol*. 2017;18(1):234. doi:10.1186/s13059-017-1362-4
21. Gabrusiewicz K, Rodriguez B, Wei J, et al. Glioblastoma-infiltrated innate immune cells resemble M0 macrophage phenotype. *JCI Insight*. 2016;1(2):e85841. doi:10.1172/jci.insight.85841
22. Pombo Antunes AR, Scheyltjens I, Lodi F, et al. Single-cell profiling of myeloid cells in glioblastoma across species and disease stage reveals macrophage competition and specialization. *Nat Neurosci*. 2021;24(4):595-610. doi:10.1038/s41593-020-00789-y
23. Chen Z, Feng X, Herting CJ, et al. Cellular and molecular identity of tumor-associated macrophages in glioblastoma. *Cancer Res*. 2017;77(9):2266-2278. doi:10.1158/0008-5472.CAN-16-2310
24. Tu S, Lin X, Qiu J, et al. Crosstalk between tumor-associated microglia/macrophages and CD8-positive T cells plays a key role in glioblastoma. *Front Immunol*. 2021;12:650105. doi:10.3389/fimmu.2021.650105
25. Batchu S, Hanafy KA, Redjal N, Godil SS, Thomas AJ. Single-cell analysis reveals diversity of tumor-associated macrophages and their interactions with T lymphocytes in glioblastoma. *Sci Rep*. 2023;13(1):20874. doi:10.1038/s41598-023-48116-2
26. Woroniecka K, Chongsathidkiet P, Rhodin K, et al. T-cell exhaustion signatures vary with tumor type and are severe in glioblastoma. *Clin Cancer Res*. 2018;24(17):4175-4186. doi:10.1158/1078-0432.CCR-17-1846
27. Waldman AD, Fritz JM, Lenardo MJ. A guide to cancer immunotherapy: from T cell basic science to clinical practice. *Nat Rev Immunol*. 2020;20(11):651-668. doi:10.1038/s41577-020-0306-5
28. Oliveira G, Wu CJ. Dynamics and specificities of T cells in cancer immunotherapy. *Nat Rev Cancer*. 2023;23(5):295-316. doi:10.1038/s41568-023-00560-y
29. M. Lauss, M. Donia, I.M. Svane, G. Jönsson, B cells and tertiary lymphoid structures: friends or foes in cancer immunotherapy?, Clinical cancer research: an official journal of the American Association for *Cancer Res*, 28 (2022) 1751–1758, 9, doi:10.1158/1078-0432.CCR-21-1130.
30. Gu S, Qian L, Zhang Y, et al. Significance of intratumoral infiltration of B cells in cancer immunotherapy: from a single cell perspective. *Biochim Biophys Acta Rev Cancer*. 2021;1876(2):188632. doi:10.1016/j.bbcan.2021.188632
31. Baig MS, Roy A, Rajpoot S, et al. Tumor-derived exosomes in the regulation of macrophage polarization. *Inflamm Res*. 2020;69(5):435-451. doi:10.1007/s00011-020-01318-0
32. Lee-Chang C, Rashidi A, Miska J, et al. Myeloid-derived suppressive cells promote B cell-mediated immunosuppression via transfer of PD-L1 in glioblastoma, cancer. *Immunol Res*. 2019;7(12):1928-1943. doi:10.1158/2326-6066.CIR-19-0240
33. Campos B, Olsen LR, Urup T, Poulsen HS. A comprehensive profile of recurrent glioblastoma. *Oncogene*. 2016;35(45):5819-5825. doi:10.1038/onc.2016.85
34. Jackson CM, Choi J, Lim M. Mechanisms of immunotherapy resistance: lessons from glioblastoma. *Nat Immunol*. 2019;20(9):1100-1109. doi:10.1038/s41590-019-0433-y

SUPPORTING INFORMATION

Additional supporting information can be found online in the Supporting Information section at the end of this article.

How to cite this article: Knudsen AM, Ewald JD, Pedersen V, Haupt-Jorgensen M, Hansen EVR, Kristensen BW. Characterisation of the tumour microenvironment in primary and recurrent glioblastomas. *Neuropathol Appl Neurobiol*. 2024;50(5):e13012. doi:10.1111/nan.13012